Sensitivity of Arctic ozone loss to polar stratospheric cloud volume and chlorine and bromine loading in a chemistry and transport model

A. R. Douglass,[1] R. S. Stolarski,[1] S. E. Strahan,[2] and B. C. Polansky[3]

Received 4 April 2006; revised 6 July 2006; accepted 1 August 2006; published 9 September 2006.

[1] The sensitivity of Arctic ozone loss to polar stratospheric cloud volume (V_{PSC}) and chlorine and bromine loading is explored using chemistry and transport models (CTMs). One simulation uses multi-decadal winds and temperatures from a general circulation model (GCM). Winter polar ozone loss depends on both equivalent effective stratospheric chlorine (EESC) and polar vortex characteristics (temperatures, descent, isolation, polar stratospheric cloud amount). The simulation reproduces a linear relationship between ozone loss and V_{PSC} in agreement with that derived from observations for 1992–2003. The relationship holds for EESC within ~85% of its maximum (~1990–2020). For lower EESC the ozone loss varies linearly with EESC unless $V_{PSC} \sim 0$. A second simulation recycles a single year's winds and temperatures from the GCM so that polar ozone loss depends only on changes in EESC. This simulation shows that ozone loss varies linearly with EESC for the entire EESC range for constant, high V_{PSC}. **Citation:** Douglass, A. R., R. S. Stolarski, S. E. Strahan, and B. C. Polansky (2006), Sensitivity of Arctic ozone loss to polar stratospheric cloud volume and chlorine and bromine loading in a chemistry and transport model, *Geophys. Res. Lett.*, *33*, L17809, doi:10.1029/2006GL026492.

1. Introduction

[2] *Rex et al.* [2004] (hereinafter referred to as R2004) report a linear relationship between winter-spring loss of Arctic ozone and the volume of polar stratospheric clouds (PSCs). R2004 used data for 10 winters between 1992 and 2003, a period when inorganic chlorine in the upper stratosphere was close to its maximum. R2004 suggest this relationship as an element of Chemistry Climate Model (CCM) evaluation and point out that additional stratospheric cooling could lead to more PSCs and additional polar ozone loss. Chemistry and transport models (CTMs) are driven by input meteorological fields and ignore feedback processes that are included in CCMs, but still should reproduce this relationship. R2004 show that the sensitivity of polar ozone loss to the volume of PSCs (V_{PSC}) in a version of the SLIMCAT CTM, driven by meteorological fields from the United Kingdom Meteorological Office UKMO, is less than that derived from observations. *Chipperfield et al.* [2005] show that a modified version of SLIMCAT reproduces the observed relationship.

[3] Here we focus on simulations using the GSFC CTM driven by meteorological output from a General Circulation Model (GCM). *Stolarski et al.* [2006] show that simulated mean total ozone for 60°S–60°N reproduces many aspects of Total Ozone Mapping Spectrometer observations. Here we show the realism of the simulated polar vortex by comparing N_2O and its horizontal gradients with N_2O observed by the Microwave Limb Sounder (MLS) on NASA's Aura satellite [*Waters et al.*, 2006]. We show that the sensitivity of simulated winter chemical loss of ozone to V_{PSC} follows the R2004 relationship for 1990–2020, years when the equivalent effective stratospheric chlorine (EESC), i.e., chlorine and bromine available in the stratosphere to destroy ozone, is within 85% of its maximum. This simulation used standard photochemical input data and a standard scenario for chlorine and bromine source gases. We also investigate the dependence of polar ozone loss on EESC for fixed V_{PSC}.

[4] Simulations use the GSFC CTM and the Global Modeling Initiative (GMI) CTM [*Douglass et al.*, 2004], described in Section 2. Section 3 shows comparisons with N_2O to support the realism of the simulated polar vortex and verifies the method used to account for the ozone increase due to transport. Results are presented in section 4 followed by discussion and conclusions.

2. Chemistry and Transport Models

[5] *Stolarski et al.* [2006] describe the GSFC CTM and the primary simulation used here. Meteorological fields from a 50-year integration of the GEOS-4 GCM (Goddard Earth Observing System, Version 4, General Circulation Model) are input to the CTM. The GCM and its implementation are described elsewhere [*Stolarski et al.*, 2006, and references therein]. Aspects of the CTM important to this analysis follow. Rate constant data and cross sections are taken from JPL Evaluation 14 [*Sander et al.*, 2003] (hereinafter referred to as JPL2003). The polar stratospheric cloud parameterization follows *Considine et al.* [2000] and accounts for denitrification through PSC sedimentation. The *Lin and Rood* [1996] constituent transport scheme is used. The horizontal grid is 2.5° longitude and 2° latitude. The 28 vertical levels between the surface and 0.4 hPa use a terrain following coordinate in the troposphere and pressure above the interface at 247 hPa. Vertical spacing is about 1 km near the tropopause and increases to 4 km near the upper boundary. Surface boundary conditions for source gases including CFCs, halons, methane and nitrous oxide are specified from Scenario A2 in Appendix 4B of the Scientific Assessment of Ozone Depletion: 2002 [*World Meteorological Organization*, 2003].

[6] A second simulation investigates the dependence of ozone loss on EESC for fixed V_{PSC}. The Global Modeling

[1]NASA Goddard Space Flight Center, Greenbelt, Maryland, USA.
[2]Goddard Earth Science and Technology Center, University of Maryland Baltimore County, Baltimore, Maryland, USA.
[3]Science Systems and Applications, Inc., Lanham, Maryland, USA.

0094-8276/06/2006GL026492$05.00

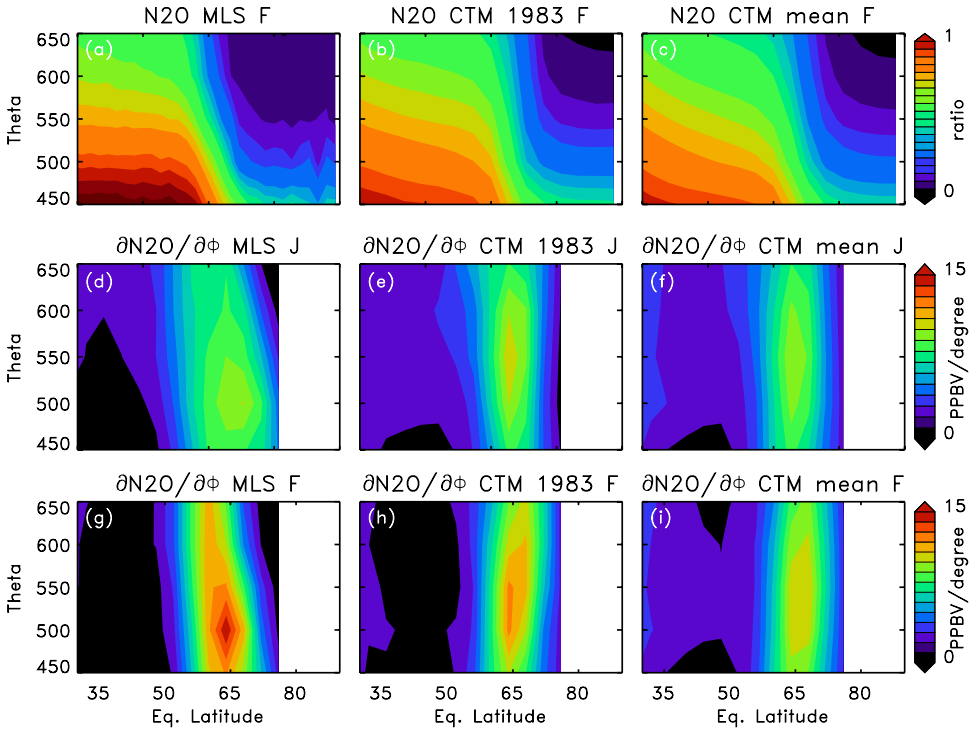

Figure 1. (top) Feb mean N_2O normalized by N_2O in the tropics at 450 K: (a) MLS, (b) GSFC CTM 1983, (c) GSFC CTM multiyear mean. (middle) Jan horizontal N_2O gradients: (d) MLS, (e) GSFC CTM 1983, (f) CTM multiyear mean. (bottom) Feb horizontal N_2O gradients: (g) MLS, (h) GSFC CTM 1983, (i) GSFC CTM multiyear mean.

Initiative CTM had already produced a simulation with identical boundary conditions using a single years' meteorology from the GCM. A year with a cold Arctic vortex had been chosen to estimate the maximum possible impact of polar ozone loss. The GMI CTM used the same chemical mechanism, rate constant and cross section data from JPL2003, the same PSC parameterization, the same numerical transport and horizontal grid resolution as the GSFC CTM [*Rotman et al.*, 2001; *Douglass et al.*, 2004]. There are 5 additional vertical levels with an upper boundary at 0.01 hPa. The GMI CTM uses SMVGEAR to solve the photochemical part of constituent continuity equations [*Jacobson*, 1995]. The V_{PSC} is nearly identical each year for recycled meteorology, varying slightly due to small changes in nitric acid. The fields from the GMI CTM are nearly identical to those obtained with the GSFC CTM for the year with the same meteorological fields and boundary conditions.

[7] A third simulation, using the GSFC CTM, is identical to the first simulation except that boundary conditions for chlorine and bromine source gases are held fixed at background levels (~1960) and its duration is 25 years (1979–2004). This simulation is used to verify our calculation of the transport contribution to winter polar ozone change.

3. Analysis

3.1. Arctic Polar Vortex

[8] Simulation of winter polar ozone loss requires realistic simulation of temperatures, size and isolation of the Arctic winter vortex. V_{PSC} as used by R2004 is a proxy for temperature, thus the realistic range for simulated V_{PSC} shown in the next section compared with that derived by R2004 implies realistic temperatures. We compare simulated N_2O with that observed by Aura MLS [*Froidevaux et al.*, 2006] to show credibility of vortex size and mixing barriers. Since the meteorological fields used in the CTM are taken from a GCM, we must select simulated years for which the meteorological fields are similar. MLS data for each month in 2005 are binned and averaged by equivalent latitude on potential temperature surfaces. The February MLS averages between 500 and 600 K are nearly constant within the polar vortex and change by less than 10 ppbv from their January values. This condition is used to select simulated winters for comparison with MLS N_2O.

[9] The binned and averaged MLS N_2O for Feb. 2005 (Figure 1a) is compared with the same average for year 10 (Figure 1b) and with the Feb. mean of 29 simulated winters that also meet this condition (Figure 1c). Year 10 of the simulation has a trace gas boundary condition corresponding to 1983. The comparison is similar for any of the 29 winters that meet the above condition for the change in N_2O. All distributions are normalized by N_2O at 450 K in the tropics to eliminate the time dependence on the boundary condition and to eliminate a systematic lower stratospheric bias in the MLS data [*Froidevaux et al.*, 2006]. The simulation reproduces low values of high-latitude N_2O observed by MLS. Comparisons of tracer gradients are more revealing [*Sankey and Shepherd*, 2003]. The location and strength of the maximum horizontal gradients in MLS N_2O for Jan. and Feb. (Figures 1d and 1g) compare well for those computed for the single simulated year for Jan. and Feb. (Figures 1e and 1h) and for 29-winter mean (Figures 1f

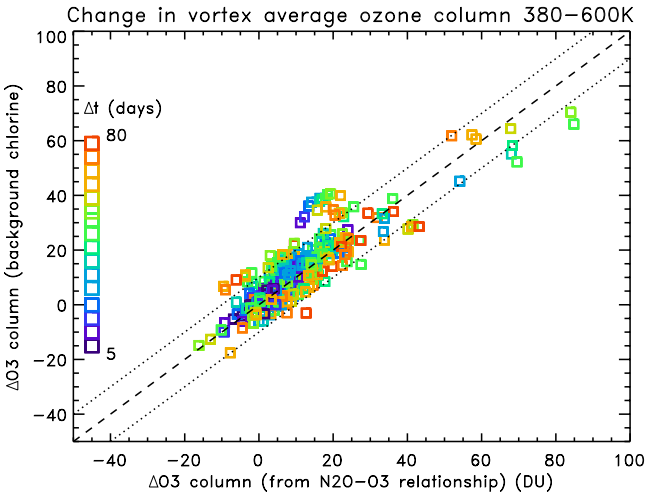

Figure 2. The increase in ozone column due to descent calculated from the N_2O-O_3 relationship versus the vortex average increase in ozone column between 380 and 600 K from a simulation with very low chlorine. Eighty-six percent of the points fall within the light dashed lines; these are ±10 DU from the 1:1 line.

and 1i), showing that the vortex size and mixing barrier are credible. As observed, the simulated February gradient maxima are stronger and equatorward of January maxima. The gradient of the mean distribution is weaker than the MLS gradient, due to interannual variability in vortex size. These comparisons show that, as observed, simulated N_2O descends from the upper stratosphere without significant horizontal mixing. Descent is necessary to obtain high values of Cly and Bry in the lower polar vortex. A strong barrier to mixing is necessary because mixing inhibits ozone loss both by decreasing Cly and Bry inside the vortex and by speeding conversion of chlorine radicals to reservoir species.

3.2. Ozone Increase Due to Transport

[10] Ozone at high northern latitudes increases due to descent during winter. This increase must be accounted for to determine the chemical ozone loss. *Harris et al.* [2002] show that consistent values for ozone loss are obtained from observations using several techniques if the altitude range, vortex-edge definition, and time periods are consistent.

[11] We determine the vortex boundary from potential vorticity [*Nash et al.*, 1996] and calculate the vortex average profiles of N_2O and O_3 between 380K and 600K for days 1, 6, 11, 16, 21 and 26 during January, February and March. We assume that the relationship between the N_2O and O_3 mean profiles does not change in the absence of chemical loss. We calculate the difference between the vortex average N_2O profile on each of these days and the profile on January 1 and use that difference to estimate the change in O_3 due to descent. We use our background chlorine simulation to test the method. There is negligible polar chemical loss of ozone for background chlorine levels, and the difference between a value of the vortex-average ozone between 380 and 600 K and its value on January 1 is the transport change for the time interval between that day and January 1. Figure 2 compares the transport change in O_3 calculated using the O_3-N_2O relationship on January 1 with that calculated from the background chlorine simulation. The colors show the time interval and change from blue to red as the interval lengthens. The scatter is similar for the different time intervals and is the same order as the 10–15 DU uncertainty in ozone loss estimated by R2004. Errors do not systematically increase as the time interval lengthens. We estimate the transport contribution using the N_2O-O_3 relationship for the remainder of this work.

3.3. Polar Stratospheric Cloud Volume

[12] R2004 estimated the volume where PSC formation is possible (V_{PSC}) using temperatures from ECMWF meteorological analyses and assumed profiles for HNO_3 and H_2O following *Hansen and Mauersberger* [1988]. In the CTM we use a similar procedure except with simulated profiles of H_2O and HNO_3. Averaged over all winters the CTM V_{PSC} exceeds that estimated by applying the method of R2004 to CTM temperatures by 30% because both H_2O and HNO_3 are slightly higher than the R2004 profiles. Although *Rex et al.* [2002] show that V_{PSC} tracks PSC observations from the Polar Ozone and Aerosol Measurement (POAM) the altitude range for observed and possible PSCs differ, suggesting uncertainty in the actual PSC volume. We know that the simulation uses the computed PSCs for heterogeneous reactions. We examine the sensitivity of computed ozone loss considering both the V_{PSC} actually used by the CTM and the estimate calculated following R2004. A few simulated winters are warm and no PSCs are formed; these years are not included when calculating the sensitivity of ozone loss to V_{PSC}.

4. Results

[13] Ozone loss is shown as a function of V_{PSC} from the CTM in Figure 3. The warm winters with $V_{PSC} \sim 0$ are not included in this figure. The center solid line is the best fit for V_{PSC} between 5 and 40 × 10^6 km^3. The slope is 2.2 ± 0.5 DU/10^6 km^3 for V_{PSC} from the CTM. This is nearly the same sensitivity as obtained by R2004 (2.1 ± 0.2 DU/10^6 km^3). The results are not sensitive to the way in which V_{PSC} is determined and a similar value (2.4 ± 0.6 DU/10^6 km^3) is obtained for V_{PSC} calculated from simulation temperatures following R2004.

[14] The chlorine and bromine source gases change greatly during the simulation and it makes sense to examine the sensitivity to the amount of chlorine and bromine

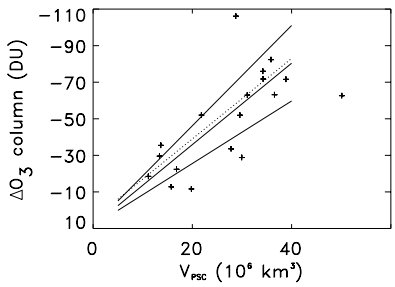

Figure 3. CTM vortex averaged chemical ozone loss versus CTM V_{PSC} for V_{PSC} greater than 5 × 10^6 km^3. The central line is the best fit; the outer lines include 1-sigma slope errors. The dashed line is the fit obtained by R2004.

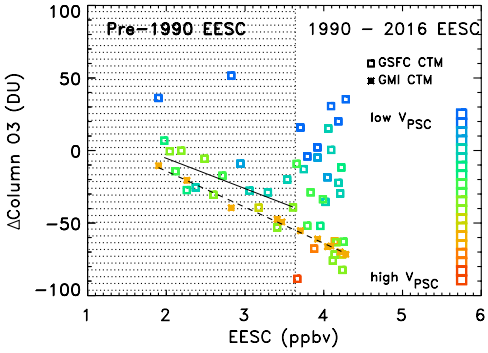

Figure 4. Ozone loss versus EESC evaluated at 1 hPa for the GSFC CTM (squares) and for the GMI CTM (asterisks). Colors show V_{PSC} ($V_{PSC} \sim 0$ blue, VPSC $\sim$ 60 red). The solid line is the best fit for GSFC CTM results for winters with ozone loss and pre-1990 EESC. The dashed line is the best fit for the GMI CTM results. The blue points with $\sim$0 V_{PSC} show positive ozone changes. These positive changes occur during warm winters when the method for calculating ozone loss breaks down and do not indicate chemical ozone production.

available for ozone destruction using EESC = Cl_y + 50* Br_y. Because winter polar vortex levels of Cl_y and Br_y track upper stratospheric levels, we evaluate EESC at 1 hPa. Figure 4 shows ozone loss from both CTMs vs. EESC; points are colored according to V_{PSC} and all winters are included. Squares are from the GSFC CTM and asterisks are from the GMI CTM. For EESC between 1.8 ppbv and $\sim$3.6 ppbv, and moderate values of V_{PSC}, the ozone loss varies linearly with EESC. The solid line in the stippled area (pre-1990 EESC) is the best fit between EESC and GSFC CTM including only winters with $V_{PSC} > 0$. For warm winters, $V_{PSC} \sim 0$ (blue), and the simulated winter ozone change is small or positive. The positive values do not imply ozone production, rather they show the assumptions used to calculate the transport contribution to ozone loss break down during warm, disturbed winters.

[15] The GMI CTM sensitivity to EESC (dashed line) nearly parallels that of the GSFC CTM. The orange points (same values of V_{PSC}) from both simulations fall on or near the dashed line. EESC reaches 85% of its maximum in $\sim$1990 and remains in that range until $\sim$2020. For this EESC range ozone loss is sensitive to V_{PSC}. Winters with low V_{PSC} (blue) have little ozone loss, those with moderate V_{PSC} (green) have moderate ozone loss, and those with high V_{PSC} (red) have substantial ozone loss. The dashed line fit to GMI results shows that ozone loss varies linearly with EESC for the entire EESC range for fixed V_{PSC}.

5. Discussion and Conclusions

[16] The GSFC simulation reproduces the slope of the empirical relationship between polar ozone loss and V_{PSC} described by R2004. *Chipperfield et al.* [2005] show that a modified version of SLIMCAT reproduces the observed empirical relationship. Modifications include improving the denitrification scheme, an updated calculation of diabatic heating, and addition of 100 pptv of chlorine and 6 pptv bromine to represent effects of very short-lived halocarbons. The *Burkholder et al.* [1990] cross sections for photolysis of Cl_2O_2 are extrapolated to long wavelengths, following *Stimpfle et al.* [2004] who show that the Cl_2O_2 loss calculated using these cross sections and the production of Cl_2O_2 calculated using JPL2003 are consistent with atmospheric observations. This leads to more ozone destruction than using cross sections recommended by JPL2003.

[17] If the latter two modifications were implemented in the GSFC CTM, its sensitivity of winter ozone loss to V_{PSC} would exceed that derived by R2002 because the rate of ozone loss would be greater due to the added chlorine and bromine and due to the faster photolysis of Cl_2O_2. It is not obvious why the sensitivity of winter polar ozone to V_{PSC} differ in the SLIMCAT CTM and the GSFC CTM when the input photochemical data and boundary conditions are the same. An important difference is that SLIMCAT uses meteorological fields from an assimilation system and the GSFC and GMI CTMs use meteorological fields from a GCM. Analysis has shown that GSFC CTM exhibits excess horizontal mixing when driven by meteorological fields from various versions of the GEOS Data Assimilation System [e.g., *Considine et al.*, 2003]. *Schoeberl et al.* [2003] use trajectory calculations to show that use of the diabatic heating for vertical motion does not improve the horizontal transport using meteorological fields from GEOS DAS or from UKMO. Simulated winter polar ozone will be less sensitive to V_{PSC} if there is any excess mixing of middle latitude air into the polar vortex, as such mixing reduces the active chlorine and bromine and also speeds re-formation of chlorine reservoirs. We suggest that evaluation of the observed and simulated sensitivity of polar ozone to V_{PSC} include a diagnostic of vortex isolation such as discussed by *Sankey and Shepherd* [2003]. Physical interpretation of agreement (or disagreement) between simulation and the R2004 diagnostic is more meaningful if the simulation can be shown to isolate the polar vortex realistically.

[18] Sensitivity of ozone loss to V_{PSC} depends on several factors, including descent, temperature, vortex isolation and photochemistry. A simulation may produce the wrong sensitivity if any of these are in error, or may produce the correct sensitivity in the case of compensating errors. Comparisons of simulations with observations provide insight into the realism of the photochemical mechanism but other aspects of simulation performance such as vortex isolation also affect comparisons. Although *Stimpfle et al.* [2004] demonstrate consistency between production, loss and observations using *Burkholder et al.* [1990] cross sections and the JPL2003 rate for Cl_2O_2 production, recent measurements of cross sections by *Pope et al.* [2005] are smaller than JPL2003, suggesting issues remain to be resolved. The ozone sensitivity to temperature calculated by any CTM depends on the Cl_2O_2 cross sections, and also on other aspects of the CTM. It is prudent that any controversy concerning recommended cross sections for atmospheric photolysis of Cl_2O_2 be resolved through analysis of laboratory results.

[19] **Acknowledgments.** We thank the Aura Microwave Limb Sounder team for their N_2O measurements. This project was supported by NASA's Atmospheric Chemistry Modeling and Analysis Program. Computing resources were provided by the NASA Center for Computational Sciences (NCCS).

References

Burkholder, J. B., J. J. Orlando, and C. J. Howard (1990), Ultraviolet absorption cross-sections of Cl_2O_2 between 210 and 410 nm, *J. Phys. Chem.*, *94*, 687–695.

Chipperfield, M. P., W. Feng, and M. Rex (2005), Arctic ozone loss and climate sensitivity: Updated three-dimensional model study, *Geophys. Res. Lett.*, *32*, L11813, doi:10.1029/2005GL022674.

Considine, D. B., A. R. Douglass, P. S. Connell, D. E. Kinnison, and D. A. Rotman (2000), A polar stratospheric cloud parameterization for the global modeling initiative three-dimensional model and its response to stratospheric aircraft, *J. Geophys. Res.*, *105*, 3955–3974.

Considine, D. B., S. R. Kawa, M. R. Schoeberl, and A. R. Douglass (2003), N_2O and NO_y observations in the 1999/2000 Arctic polar vortex: Implications for transport processes in a CTM, *J. Geophys. Res.*, *108*(D5), 4170, doi:10.1029/2002JD002525.

Douglass, A. R., R. S. Stolarski, S. E. Strahan, and P. S. Connell (2004), Radicals and reservoirs in the GMI chemistry and transport model: Comparison to measurements, *J. Geophys. Res.*, *109*, D16302, doi:10.1029/2004JD004632.

Froidevaux, L., et al. (2006), Early validation analyses of atmospheric profiles form EOS MLS on the Aura satellite, *IEEE Trans. Geosci. Remote Sens.*, *44*, 1106–1121.

Hansen, D. R., and K. Mauersberger (1988), Laboratory studies of the nitric acid trihydrate: Implications for the south polar stratosphere, *Geophys. Res. Lett.*, *15*, 855–858.

Harris, N. R. P., M. Rex, F. Goutail, B. M. Knudsen, G. L. Manney, R. Müller, and P. von der Gathen (2002), Comparison of empirically derived ozone losses in the Arctic vortex, *J. Geophys. Res.*, *107*(D20), 8264, doi:10.1029/2001JD000482.

Jacobson, M. Z. (1995), Computation of global photochemistry with SMVGEAR II, *Atmos. Environ.*, *29*, 2541–2546.

Lin, S.-J., and R. B. Rood (1996), Multidimensional flux form semi-Lagrangian transport schemes, *Mon. Weather Rev.*, *124*, 2046–2070.

Nash, E. R., P. A. Newman, J. E. Rosenfield, and M. R. Schoeberl (1996), An objective determination of the polar vortex using Ertel's potential vorticity, *J. Geophys. Res.*, *101*, 9471–9478.

Pope, F. D., J. C. Hansen, K. D. Bayes, R. R. Friedl, and S. P. Sander (2005), Re-determination of the UV absorption cross sections of ClOOCl, *Eos Trans. AGU*, *86*(52), Fall Meet. Suppl., Abstract A13D-0970.

Rex, M., et al. (2002), Chemical depletion of Arctic ozone in winter 1999/2000, *J. Geophys. Res.*, *107*(D20), 8276, doi:10.1029/2001JD000533.

Rex, M., R. J. Salawitch, P. von der Gathen, N. R. P. Harris, M. P. Chipperfield, and B. Naujokat (2004), Arctic ozone loss and climate change, *Geophys. Res. Lett.*, *31*, L04116, doi:10.1029/2003GL018844.

Rotman, D. A., et al. (2001), Global Modeling Initiative assessment model: Model description, integration, and testing of the transport shell, *J. Geophys. Res.*, *106*, 1669–1691.

Sander, S. P., et al. (Eds.) (2003), Chemical kinetics and photochemical data for use in atmospheric studies, *JPL Publ., 02–25*.

Sankey, D., and T. G. Shepherd (2003), Correlations of long-lived chemical species in a middle atmosphere general circulation model, *J. Geophys. Res.*, *108*(D16), 4494, doi:10.1029/2002JD002799.

Schoeberl, M. R., A. R. Douglass, Z. Zhu, and S. Pawson (2003), A comparison of the lower stratospheric age spectra derived from a general circulation model and two data assimilation systems, *J. Geophys. Res.*, *108*(D3), 4113, doi:10.1029/2002JD002652.

Stimpfle, R. M., D. M. Wilmouth, R. J. Salawitch, and J. G. Anderson (2004), First measurements of ClOOCl in the stratosphere: The coupling of ClOOCl and ClO in the Arctic polar vortex, *J. Geophys. Res.*, *109*, D03301, doi:10.1029/2003JD003811.

Stolarski, R. S., A. R. Douglass, S. Steenrod, and S. Pawson (2006), Trends in stratospheric ozone: Lessons learned from a 3D chemistry transport model, *J. Atmos. Sci.*, *63*, 1028–1041.

Waters, J., et al. (2006), The Earth Observing System Microwave Limb Sounder (EOS MLS) on the Aura satellite, *IEEE Trans. Geosci. Remote Sens.*, *44*, 1075–1092.

World Meteorological Organization (2003), Scientific assessment of ozone depletion: 2002, *Global Ozone Res. Monit. Proj. Rep. 47*, Geneva, Switzerland.

A. R. Douglass and R. S. Stolarski, Atmospheric Chemistry and Dynamics Branch, NASA Goddard Space Flight Center, Code 613.3, Greenbelt, MD 20771, USA. (anne.r.douglass@nasa.gov)

B. C. Polansky, Science Systems Applications, Inc., 10210 Greenbelt Road, Suite 600, Lanham, MD 20706, USA.

S. E. Strahan, Goddard Earth Science and Technology Center, University of Maryland Baltimore County, 5523 Research Park Drive, Suite 320, Baltimore, MD 21228, USA.